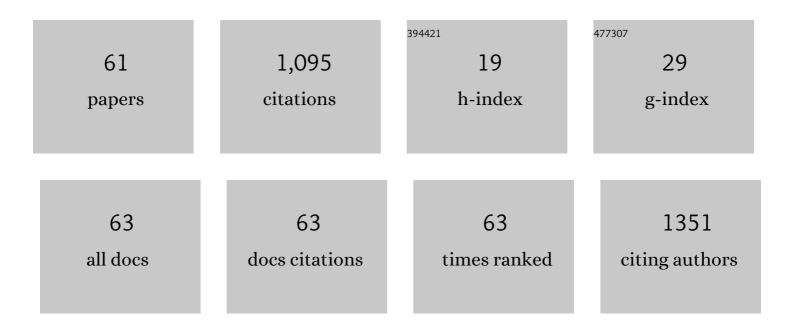
Mengliang Zhang

List of Publications by Year in descending order

Source: https://exaly.com/author-pdf/452464/publications.pdf Version: 2024-02-01



#	Article	IF	CITATIONS
1	The left-right side-specific endocrine signaling: implications for neurological deficits in stroke and neurodevelopmental disorders. Neural Regeneration Research, 2022, 17, 2431.	3.0	1
2	Development of a Metabolite Ratio Rule-Based Method for Automated Metabolite Profiling and Species Differentiation of Four Major Cinnamon Species. Journal of Agricultural and Food Chemistry, 2022, 70, 5450-5457.	5.2	2
3	The Development of Hindlimb Postural Asymmetry Induced by Focal Traumatic Brain Injury Is Not Related to Serotonin 2A/C Receptor Expression in the Spinal Cord. International Journal of Molecular Sciences, 2022, 23, 5358.	4.1	0
4	MIF in the cerebrospinal fluid is decreased during relapsing-remitting while increased in secondary progressive multiple sclerosis. Journal of the Neurological Sciences, 2022, 439, 120320.	0.6	5
5	The levels of the serine protease HTRA1 in cerebrospinal fluid correlate with progression and disability in multiple sclerosis. Journal of Neurology, 2021, 268, 3316-3324.	3.6	6
6	Left-Right Side-Specific Neuropeptide Mechanism Mediates Contralateral Responses to a Unilateral Brain Injury. ENeuro, 2021, 8, ENEURO.0548-20.2021.	1.9	10
7	Unilateral traumatic brain injury of the left and right hemisphere produces the left hindlimb response in rats. Experimental Brain Research, 2021, 239, 2221-2232.	1.5	6
8	Unilateral brain injury to pregnant rats induces asymmetric neurological deficits in the offspring. European Journal of Neuroscience, 2021, 53, 3621-3633.	2.6	4
9	Left-right side-specific endocrine signaling complements neural pathways to mediate acute asymmetric effects of brain injury. ELife, 2021, 10, .	6.0	9
10	Vibronic Excitons and Conical Intersections in Semiconductor Quantum Dots. Journal of Physical Chemistry Letters, 2021, 12, 9677-9683.	4.6	5
11	Rapid and Sensitive Identification and Discrimination of Bound/Unbound Ligands on Colloidal Nanocrystals via Direct Analysis in Real-Time Mass Spectrometry. Langmuir, 2021, 37, 14703-14712.	3.5	3
12	Forensic Fiber Analysis by Thermal Desorption/Pyrolysis-Direct Analysis in Real Time-Mass Spectrometry. Analytical Chemistry, 2020, 92, 1925-1933.	6.5	20
13	Hindlimb motor responses to unilateral brain injury: spinal cord encoding and left-right asymmetry. Brain Communications, 2020, 2, fcaa055.	3.3	15
14	Ipsilesional <i>versus</i> contralesional postural deficits induced by unilateral brain trauma: a side reversal by opioid mechanism. Brain Communications, 2020, 2, fcaa208.	3.3	14
15	Detection and Classification of Ignitable Liquid Residues in the Presence of Matrix Interferences by Using Direct Analysis in Real Time Mass Spectrometry,. Journal of Forensic Sciences, 2019, 64, 1486-1494.	1.6	23
16	The classification of Cannabis hemp cultivars by thermal desorption direct analysis in real time mass spectrometry (TD-DART-MS) with chemometrics. Analytical and Bioanalytical Chemistry, 2019, 411, 8133-8142.	3.7	14
17	Discrimination of brands of gasoline by using DART-MS and chemometrics. Forensic Chemistry, 2018, 10, 58-66.	2.8	28
18	Antitumor and immunomodulatory activities of total flavonoids extract from persimmon leaves in H22 liver tumor-bearing mice. Scientific Reports, 2018, 8, 10523.	3.3	22

MENGLIANG ZHANG

#	Article	IF	CITATIONS
19	A computational tool for accelerated analysis of oligomeric proanthocyanidins in plants. Journal of Food Composition and Analysis, 2017, 56, 124-133.	3.9	9
20	Feruloyl dopamine-O-hexosides are efficient marker compounds as orthogonal validation for authentication of black cohosh (Actaea racemosa)—an UHPLC-HRAM-MS chemometrics study. Analytical and Bioanalytical Chemistry, 2017, 409, 2591-2600.	3.7	16
21	MS ^{All} strategy for comprehensive quantitative analysis of PEGylated-doxorubicin, PEG and doxorubicin by LC-high resolution q-q-TOF mass spectrometry coupled with all window acquisition of all fragment ion spectra. Analyst, The, 2017, 142, 4279-4288.	3.5	17
22	Development of a Comprehensive Flavonoid Analysis Computational Tool for Ultrahigh-Performance Liquid Chromatography-Diode Array Detection-High-Resolution Accurate Mass-Mass Spectrometry Data. Analytical Chemistry, 2017, 89, 7388-7397.	6.5	22
23	Heterogenic Distribution of Aromatic L-Amino Acid Decarboxylase Neurons in the Rat Spinal Cord. Frontiers in Integrative Neuroscience, 2017, 11, 31.	2.1	8
24	GLS-Finder: A Platform for Fast Profiling of Glucosinolates in <i>Brassica</i> Vegetables. Journal of Agricultural and Food Chemistry, 2016, 64, 4407-4415.	5.2	27
25	Comprehensive characterization of <i>C</i> -glycosyl flavones in wheat (<i>Triticum aestivum</i> L.) germ using UPLC-PDA-ESI/HRMS ⁿ and mass defect filtering. Journal of Mass Spectrometry, 2016, 51, 914-930.	1.6	80
26	Field Analysis of Polychlorinated Biphenyls (PCBs) in Soil Using Solid-Phase Microextraction (SPME) and a Portable Gas Chromatography–Mass Spectrometry System. Applied Spectroscopy, 2016, 70, 785-793.	2.2	23
27	Production of Dopamine by Aromatic I-Amino Acid Decarboxylase Cells after Spinal Cord Injury. Journal of Neurotrauma, 2016, 33, 1150-1160.	3.4	14
28	Differentiation of <i>Aurantii fructus immaturus</i> and <i>Fructus poniciri trifoliatae immaturus</i> by Flow-Injection with Ultraviolet Spectroscopic Detection and Proton Nuclear Magnetic Resonance Using Partial Least-Squares Discriminant Analysis. Analytical Letters, 2016, 49, 711-722.	1.8	5
29	Two-step production of monoamines in monoenzymatic cells in the spinal cord: a different control strategy of neurotransmitter supply?. Neural Regeneration Research, 2016, 11, 1904.	3.0	9
30	Application of chemometrics to resolve overlapping mass spectral peak clusters between trichloroethylene and its deuterated internal standard. Rapid Communications in Mass Spectrometry, 2015, 29, 789-794.	1.5	8
31	Spinal Cord Hemisection Facilitates Aromatic L-Amino Acid Decarboxylase Cells to Produce Serotonin in the Subchronic but Not the Chronic Phase. Neural Plasticity, 2015, 2015, 1-10.	2.2	8
32	FlavonQ: An Automated Data Processing Tool for Profiling Flavone and Flavonol Glycosides with Ultra-High-Performance Liquid Chromatography–Diode Array Detection–High Resolution Accurate Mass–Mass Spectrometry. Analytical Chemistry, 2015, 87, 9974-9981.	6.5	26
33	Use of fuzzy chromatography mass spectrometric (FCMS) fingerprinting and chemometric analysis for differentiation of whole-grain and refined wheat (T. aestivum) flour. Analytical and Bioanalytical Chemistry, 2015, 407, 7875-7888.	3.7	12
34	Simultaneous quantification of Aroclor mixtures in soil samples by gas chromatography/mass spectrometry with solid phase microextraction using partial least-squares regression. Chemosphere, 2015, 118, 187-193.	8.2	14
35	Aromatic L-amino acid decarboxylase cells in the spinal cord: a potential origin of monoamines. Neural Regeneration Research, 2015, 10, 715.	3.0	7
36	Determination of Aroclor 1260 in soil samples by gas chromatography with mass spectrometry and solid-phase microextraction. Journal of Separation Science, 2014, 37, 2751-2756.	2.5	8

MENGLIANG ZHANG

#	Article	IF	CITATIONS
37	Spinal Cord Injury Enables Aromatic l-Amino Acid Decarboxylase Cells to Synthesize Monoamines. Journal of Neuroscience, 2014, 34, 11984-12000.	3.6	34
38	Comparison of Three Algorithms for the Baseline Correction of Hyphenated Data Objects. Analytical Chemistry, 2014, 86, 9050-9057.	6.5	19
39	Automated pipeline for classifying Aroclors in soil by gas chromatography/mass spectrometry using modulo compressed two-way data objects. Talanta, 2013, 117, 483-491.	5.5	16
40	Rhythmic activity of feline dorsal and ventral spinocerebellar tract neurons during fictive motor actions. Journal of Neurophysiology, 2013, 109, 375-388.	1.8	32
41	Control and Role of Plateau Potential Properties in the Spinal Cord. Current Pharmaceutical Design, 2013, 19, 4357-4370.	1.9	21
42	LC–MS–MS Determination of Troxerutin in Plasma and Its Application to a Pharmacokinetic Study. Chromatographia, 2011, 73, 165-169.	1.3	14
43	Simultaneous Determination of Escin Ia and Its Isomer Isoescin Ia by LC–MS–MS: Application to a Pharmacokinetic Study of Escin Ia in Rats. Chromatographia, 2011, 74, 243-250.	1.3	1
44	Robust upregulation of serotonin 2A receptors after chronic spinal transection of rats: An immunohistochemical study. Brain Research, 2010, 1320, 60-68.	2.2	43
45	Simultaneous analysis of isomers of escin saponins in human plasma by liquid chromatography–tandem mass spectrometry: Application to a pharmacokinetic study after oral administration. Journal of Chromatography B: Analytical Technologies in the Biomedical and Life Sciences. 2010. 878. 861-867.	2.3	18
46	Simultaneous quantitation of hydrochlorothiazide and metoprolol in human plasma by liquid chromatography–tandem mass spectrometry. Journal of Pharmaceutical and Biomedical Analysis, 2010, 52, 149-154.	2.8	39
47	Expression of calcium channel Ca _V 1.3 in cat spinal cord: Light and electron microscopic immunohistochemical study. Journal of Comparative Neurology, 2008, 507, 1109-1127.	1.6	28
48	MI Neuronal Responses to Peripheral Whisker Stimulation: Relationship to Neuronal Activity in SI Barrels and Septa. Journal of Neurophysiology, 2008, 100, 50-63.	1.8	53
49	Localization of L-type calcium channel CaV1.3 in cat lumbar spinal cord – with emphasis on motoneurons. Neuroscience Letters, 2006, 407, 42-47.	2.1	25
50	Intercolumnar synchronization of neuronal activity in rat barrel cortex during patterned airjet stimulation: a laminar analysis. Experimental Brain Research, 2006, 169, 311-325.	1.5	17
51	Stimulus-Induced Intercolumnar Synchronization of Neuronal Activity in Rat Barrel Cortex: A Laminar Analysis. Journal of Neurophysiology, 2004, 92, 1464-1478.	1.8	22
52	Lateral cervical nucleus projections to periaqueductal gray matter in cat. Journal of Comparative Neurology, 2004, 471, 434-445.	1.6	10
53	Septal columns in rodent barrel cortex: Functional circuits for modulating whisking behavior. Journal of Comparative Neurology, 2004, 480, 299-309.	1.6	60
54	Central projections of sensory innervation of the rat superficial temporal artery. Brain Research, 2003, 966, 126-133.	2.2	35

MENGLIANG ZHANG

#	Article	IF	CITATIONS
55	Organization of the ferret lateral cervical nucleus and cervicothalamic tract. Somatosensory & Motor Research, 2002, 19, 36-48.	0.9	7
56	Spinal Sensorimotor Transformation: Relation between Cutaneous Somatotopy and a Reflex Network. Journal of Neuroscience, 2002, 22, 8170-8182.	3.6	59
57	Pervasive synchronization of local neural networks in the secondary somatosensory cortex of cats during focal cutaneous stimulation. Experimental Brain Research, 2002, 147, 227-242.	1.5	15
58	Morphological features of cat cervicothalamic tract terminations in different target regions. Brain Research, 2001, 890, 280-286.	2.2	3
59	Cervicothalamic tract termination: a reexamination and comparison with the distribution of monoclonal antibody Cat-301 immunoreactivity in the cat. Anatomy and Embryology, 1998, 198, 451-472.	1.5	9
60	The cervicothalamic tract terminates in Cat301-sparse regions of the cat VPL. NeuroReport, 1996, 7, 1493-1496.	1.2	5
61	Normal Distribution and Plasticity of Serotonin Receptors after Spinal Cord Injury and Their Impacts on Motor Outputs. , 0, , .		8